

# Spatial Pileup Considerations for Pixellated Gamma-ray Detectors

L.R. Furenlid, E. Clarkson, D.G. Marks and H.H. Barrett

Department of Radiology and Optical Sciences Center  
University of Arizona, Tucson, Arizona 85724

## Abstract

High-spatial-resolution solid-state detectors being developed for gamma-ray applications benefit from having pixel dimensions substantially smaller than detector slab thickness. This leads to an enhanced possibility of charge partially spreading to neighboring pixels as a result of diffusion (and secondary photon emission) transverse to the drift direction. An undesirable consequence is the effective magnification of the event "size" and the spatial overlap issues which result when two photons are absorbed in close proximity within the integration time of the detector/readout system.

In this work, we develop the general statistics of spatial pileup in imaging systems and apply the results to detectors we are developing based on pixellated cadmium zinc telluride (CdZnTe) and a multiplexing application-specific integrated circuit (ASIC) readout. We consider the limitations imposed on total count rate capacity and explore in detail the consequences for the LISTMODE data-acquisition strategy. Algorithms are proposed for identifying and, where possible, resolving overlapping events by maximum-likelihood estimation. The efficacy and noise tolerance of these algorithms will be tested with a combination of simulated and experimental data in future work.

## I. INTRODUCTION

In prior work it has been demonstrated that the deleterious effects of poor hole transport due to charge trapping in semiconductors suitable for gamma ray detectors are largely remedied if the pixel dimensions are made small relative to the thickness of the detector slab [1]. This is a direct result from the electrostatics of the signal induction process and is sometimes known as the "small-pixel effect" [2]. It leads to the successful application of CdZnTe patterned with an array of readout electrodes as an imaging detector suitable for use in gamma-ray cameras [3-5].

Small pixel dimensions lead, however, to increased sensitivity to charge spreading due to diffusion and secondary photon emission transverse to the drift direction. As a result, the charge in a local pixel neighborhood must be summed in order to recover an acceptable energy resolution. In our detectors, which employ a 380 micron pixel pitch on a ~2 mm thick CZT wafer, inclusion of a 3×3 or 5×5 neighborhood centered on the photon interaction location yields a dramatic improvement in the obtained energy spectrum [6]. Furthermore, the additional observations

permit the estimation of the interaction location with subpixel precision, and even of the depth of interaction [7].

The principal negative consequence of charge spreading, is the more rapid onset of spatial pileup, the overlapping of the pixel neighborhoods of multiple photon events occurring within the effective integration time of the detector/readout system. Events identified to have some degree of overlap can be handled in one of two ways: they can be discarded, which results in a loss of effective count rate and a reduction in image contrast; or an effort can be made to resolve the contributing individual events via statistical estimation. For quantitative applications such as computed tomography, the introduction of a bias by discarding events (more pileups occur in brightly illuminated areas of the detector) is undesirable.

In this work, we first evaluate the severity of the spatial pileup problem as a function of count rate, and then propose algorithms for identifying and separating overlapping events.

## II. SPATIAL PILEUP STATISTICS

We first derive a quite general formulation for the probability density which describes the distribution of distances between "events" occurring in a two-dimensional detector of arbitrary shape when illuminated with an arbitrary intensity distribution. We then consider the special case of a square detector subjected to a uniform illumination of gamma-rays. Pileup versus count rate statistics relevant to our detector systems are computed, and their accuracy is confirmed with Monte Carlo simulations.

### A. Pileup Probability

In a detector subtending area  $\mathbf{A}$ , illuminated with a stationary (i.e. time independent) flux  $f(\mathbf{r})$ , the differential probability of absorption of a photon at  $\mathbf{r}$  in area  $d\alpha$  in time  $dt$  is given by

$$dP(\mathbf{r}) = \frac{f(\mathbf{r})}{\int_{\mathbf{T}} \int_{\mathbf{A}} f(\mathbf{r}) d^2 r dt} d\alpha dt. \quad (1)$$

For a detector that collects photons for some integration period  $T$  before being read out and reset, we can write a photon probability density in terms of the fluence  $\phi(\mathbf{r})$  (photons per unit area) by carrying out the integrals over time

$$\Phi(\mathbf{r}) = \frac{\phi(\mathbf{r})}{\int_{\mathbf{A}} \phi(\mathbf{r}) d^2 r}. \quad (2)$$

We can incorporate the detector shape by requiring that the effective normalized fluence  $\Phi(\mathbf{r})$  have the properties

$$\begin{aligned} \iint_{\infty} \Phi(\mathbf{r}) d^2 r &= 1 \\ \Phi(\mathbf{r}) &= 0 \text{ if } \mathbf{r} \notin \mathbf{A}, \end{aligned} \quad (3)$$

i.e., vanishes if  $\mathbf{r}$  is not a point on the detector. If we define a cylinder function  $cyl_R(\mathbf{r})$  such that

$$cyl_R(\mathbf{r}) = \begin{cases} 1 & \text{if } |\mathbf{r}| \leq R \\ 0 & \text{if } |\mathbf{r}| > R \end{cases} \quad (4)$$

the probability that a photon will land on the detector within a circle of radius  $R$  centered at  $\mathbf{r}_0$  is:

$$P_{r \leq R}(\mathbf{r}_0) = \iint_{\infty} cyl_R(\mathbf{r} - \mathbf{r}_0) \Phi(\mathbf{r}) d^2 r. \quad (5)$$

By making use of (3), the limits of integration have been extended over the entire real plane [7].

The probability that a photon will land within the circle of radius  $R + \Delta R$  and outside the circle of radius  $R$ , both centered at  $\mathbf{r}_0$  is

$$\begin{aligned} P_{R < r \leq R + \Delta R}(\mathbf{r}_0) &= \iint_{\infty} cyl_{R + \Delta R}(\mathbf{r} - \mathbf{r}_0) \Phi(\mathbf{r}) d^2 r - \\ &\iint_{\infty} cyl_R(\mathbf{r} - \mathbf{r}_0) \Phi(\mathbf{r}) d^2 r \end{aligned} \quad (6)$$

which in the limit of  $\Delta R \rightarrow 0$  gives

$$\lim_{\Delta R \rightarrow 0} \frac{P_{R < r \leq R + \Delta R}(\mathbf{r}_0)}{\Delta R} = \frac{d}{dR} \iint_{\infty} cyl_R(\mathbf{r} - \mathbf{r}_0) \Phi(\mathbf{r}) d^2 r. \quad (7)$$

The probability that two photons will be separated by a distance that is between  $R$  and  $R + \Delta R$  is given by the joint probability of a photon at  $\mathbf{r}_0$  together with a second photon the appropriate distance away as given by (7), integrated over all locations  $\mathbf{r}_0$

$$\begin{aligned} \lim_{\Delta R \rightarrow 0} \frac{P(R < r \leq R + \Delta R)}{\Delta R} &= p(R) = \\ &\iint_{\infty} \left[ \frac{d}{dR} \iint_{\infty} cyl_R(\mathbf{r} - \mathbf{r}_0) \Phi(\mathbf{r}) d^2 r \right] \Phi(\mathbf{r}_0) d^2 r_0. \end{aligned} \quad (8)$$

Equation (8) may be solved for  $p(R)$ , the probability density on interevent distances, to give

$$\begin{aligned} p(R) &= \frac{d}{dR} \iint_{\infty} \iint_{\infty} cyl_R(\mathbf{r} - \mathbf{r}_0) \Phi(\mathbf{r}) \Phi(\mathbf{r}_0) d^2 r d^2 r_0 \\ &= \frac{d}{dR} \iint_{\infty} |\Phi(\boldsymbol{\rho})|^2 \frac{RJ_1(2\pi\rho R)}{\rho} d^2 \rho \end{aligned} \quad (9)$$

where we have made use of the generalized Parseval's theorem, and the Fourier transforms

$$\mathcal{F}\{\Phi(\mathbf{r})\} = \Phi(\boldsymbol{\rho})$$

$$\mathcal{F}\{cyl_R(\mathbf{r})\} = \frac{RJ_1(2\pi\rho R)}{\rho}, \quad \rho = |\boldsymbol{\rho}|. \quad (10)$$

Carrying out the derivative in (9) leads to the final expression for the interevent distance probability density as an integral over all spatial frequencies of the product of the power spectrum of the fluence/detector function and a zeroth order Bessel function:

$$p(R) = 2\pi R \iint_{\infty} |\Phi(\boldsymbol{\rho})|^2 J_0(2\pi\rho R) d^2 \rho. \quad (11)$$

$p(R)$  is a true probability density, and it may be used, for example, to calculate the probability that two photons on the detector are within a distance  $D$  of each other by

$$P(|\Delta\mathbf{r}| \leq D) = \int_0^D p(R) dR. \quad (12)$$

From (12) it is an easy exercise to derive various statistics. For example, the expectation value for the number of photons which will be corrupted by spatial pileup (having one or more photons within  $D_{pu}$ ) if there are  $N$  photons striking the detector during an integration interval is given by

$$\langle N_{pu} \rangle = N \left[ 1 - \left( 1 - P(|\Delta\mathbf{r}| \leq D_{pu}) \right)^{N-1} \right]. \quad (13)$$

Equations (11), (12), and (13) are completely general for a position-sensitive planar detector, making no assumptions regarding the fluence function, the detector shape, or the distance limit within which "events" interfere. They are equally applicable to photographic films, particle detectors, and semiconductor-based photon detectors.

## B. Uniformly Illuminated Square Detector

In the special case of a uniformly illuminated detector of square geometry with side of length  $l$ , the fluence/detector function can be written as

$$\Phi(\mathbf{r}) = \frac{1}{l^2} \text{rect}\left(\frac{x}{l}\right) \text{rect}\left(\frac{y}{l}\right) \quad (14)$$

where

$$\text{rect}(x) = \begin{cases} 1 & \text{if } |x| \leq \frac{1}{2} \\ 0 & \text{if } |x| > \frac{1}{2} \end{cases}. \quad (15)$$

Then

$$\Phi(\boldsymbol{\rho}) = \mathcal{F}\{\Phi(\mathbf{r})\} = \frac{1}{l^2} \text{sinc}(l\rho_x) \text{sinc}(l\rho_y) \quad (16)$$

and

$$p(R) = \frac{2\pi R}{l^2} \iint_{-\infty}^{\infty} \text{sinc}^2(l\rho_x) \text{sinc}^2(l\rho_y) J_0(2\pi\rho R) d\rho_x d\rho_y \quad (17)$$

$$\rho = \sqrt{\rho_x^2 + \rho_y^2}$$

A more convenient form of (15) can be written with the introduction of the dimensionless variable  $R/l$  which remaps the interevent distance probability density into units of the detector side length

$$p(\hat{R}) = p\left(\frac{R}{l}\right) = \frac{2\pi}{l} \hat{R} \iint_{-\infty}^{\infty} \text{sinc}^2(\eta_x) \text{sinc}^2(\eta_y) J_0(2\pi\hat{R}\eta) d\eta_x d\eta_y \quad (18)$$

where

$$\eta_x = l\rho_x, \quad \eta_y = l\rho_y, \quad \text{and} \quad \eta = \sqrt{\eta_x^2 + \eta_y^2}. \quad (19)$$

We evaluated equation (18) numerically, though the existence of an analytic solution has not been excluded. Closed form solutions can be derived for other selected detector shapes.

This probability density depends only on the square shape of the detector and the assumption of even illumination, and thus can give pileup statistics for any pixel neighborhood size and count rate. The solid line in Figure 1 shows the probability density versus distance normalized to the detector side length.

### C. Monte Carlo Simulations

A Monte Carlo simulation and verification of the derived probability density function was carried out by histogramming the interevent distances resulting from random placement of photons on a  $64 \times 64$  pixel detector grid. The example plotted as points in Figure 1 was generated by 10000 simulated photons deposited in 200 frames of 50 photons each, though there is no count rate dependence as long as there are at least two photons per frame. Some apparent "noise" in the simulated data results from the discretization of the detector grid.

The curve was used to compute the predicted number of overlaps when each event occupies a  $3 \times 3$  pixel neighborhood by integrating the probability density in Figure 1 from 0 to the pileup diameter and invoking equation (13). Figure 2 illustrates the expectation value for the number of spatial pileups for our  $64 \times 64$  pixel array detector as a function of counts per frame. A comparison is again made with results from a Monte Carlo simulation (with 250 frames at each count rate) and quantitative agreement is found. As the count rate increases, the curve asymptotically approaches the limiting line with unity slope in which every photon has pileup. A different event size results in a different member of a family of curves which all have the same general shape.

The total count rate an integrating detector can accommodate is a function not only of the maximum tolerable counts per frame, of course, but also the frame rate. As our CdZnTe detectors are read and cleared once per millisecond, total count rates of at least 50-60 kCps appear feasible. These are more than adequate for advanced SPECT applications.

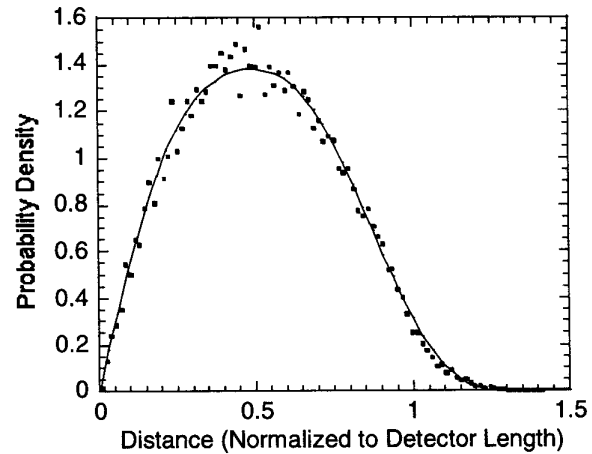


Figure 1. Computed probability density function (line) and Monte Carlo simulation (points) of the interevent distances for a uniformly illuminated square detector of arbitrary size.

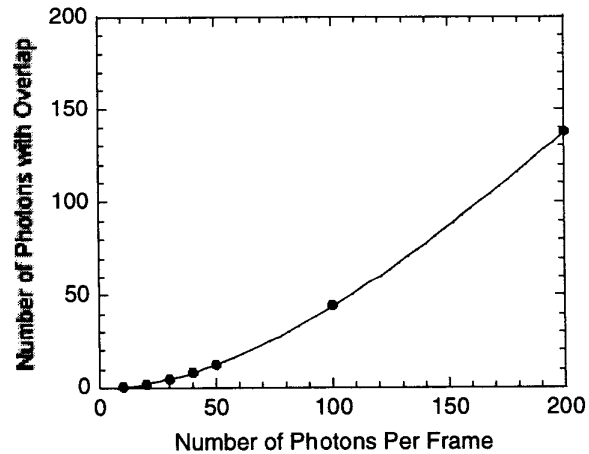


Figure 2. Computed expectation value (line) for the number of photons with pileup as a function of the number of photons per frame when each photon occupies a  $3 \times 3$  pixel neighborhood on a  $64 \times 64$  pixel array detector. Monte Carlo simulation (points) agrees quantitatively.

### III. RESOLVING OVERLAPPING EVENTS

We consider next the nature of the spatial pileups possible on a detector with discrete pixels arranged in a square array. For example, if each photon generates signal in a  $3 \times 3$  neighborhood of pixels, there are only six possible unique overlapping geometries as shown in Figure 3 in order of decreasing "interference". This means that the task of processing a set of pixel signals to obtain energy and position information with overlapping photons could be considered as one of energy estimation and pileup "type" classification. Any algorithm proposed to resolve pileups will thus need to include an overlap detection scheme as well as joint statistical estimation of energy and position.



Figure 3. The unique spatial pileups possible with  $3 \times 3$  pixel arrays.

#### A. The LISTMODE Data Collection Scheme

The advantages of LISTMODE data collection, the recording of the full set of observations associated with a data event as an entry in an ordered list, have been demonstrated in prior work [9-10]. For our pixellated gamma-ray detectors, each entry in the data list corresponds to a detected photon and might consist of a frame number, coordinates describing the location of the central pixel and the nine signal values present in the  $3 \times 3$  pixel neighborhood. The list is generated by a software (or hardware) LISTMODE "engine" which scans a frame of detector data looking for photon events, extracts the relevant set of observations, and appends the resulting entry to the data list. Statistical methods applied to estimate energy and position thus have access to the data observations at their full collected precision.

#### B. Event Detection

The simplest method for photon event detection is simply to compare each pixel signal against a threshold. In order not to miss events occurring close to an edge or corner boundary between pixels the threshold must be set quite low, nominally at less than one fourth the expected signal for the minimum photon energy. However, the superposition of signals in overlapping events then tends to elevate multiple pixels above threshold and gives rise to an inefficient condition of many more event indications than photons.

An attractive alternative is to detect photon events by performing a 2D cross-correlation operation with a  $3 \times 3$  pixel, center-weighted, template function. By selecting an

appropriate set of weights and a higher threshold, the number of LISTMODE entries will more closely match the number of actual events. Overlapped photons will still produce a small number of extra entries. Monte Carlo simulations suggest that the parameters can be adjusted to yield no more than 20% excess at 50 photons per frame in the gamma-ray detector with a  $64 \times 64$  pixel array. The presence of events with pileup is, of course, easily identified from the cluster of list entries with central pixel locations in close proximity.

#### C. Pileup Separation

An algorithm for resolving overlapped events is being developed. When a cluster of entries is discovered in the data list, the observations will be employed as the data in a maximum-likelihood joint estimate of the photon energies and locations. The specific pattern of entries generated by the cross-correlation technique can serve as the entry point in an ML search or an expectation-maximum (EM) refinement.

We can write the mean signal induced in a pixel  $j$  at location  $\mathbf{r}_j$  by a photon of energy  $E_i$  absorbed at location  $\mathbf{r}_i = (x_i, y_i)$  and depth  $z_i$  in terms of a response function  $f$  as

$$\bar{\sigma}_{i,j} = f(E_i, \mathbf{r}_i - \mathbf{r}_j, z_i) \approx \frac{E_i}{E_0} f_0(\mathbf{r}_i - \mathbf{r}_j, z_i). \quad (20)$$

If there are  $N$  overlapping photons contributing to the pixel signal and a superposition principle is valid (true for our charge integrating multiplexer readouts), then the final observed signal in pixel  $j$  can be written as

$$s_j = \sum_{i=1}^N \bar{\sigma}_{i,j}. \quad (21)$$

If we are extracting  $3 \times 3$  pixel neighborhoods as LISTMODE entries associated with each detected event, then each entry will comprise a data vector  $\mathbf{S}_k$  with nine components

$$\mathbf{S}_k = [s_{k-65}, s_{k-64}, s_{k-63}, s_{k-62}, s_{k-61}, s_{k-60}, s_{k-59}, s_{k-58}, s_{k-57}], \quad (22)$$

where we have enumerated each pixel in our  $64 \times 64$  array by a single index  $k$  running row by row from 0 to 4095 [11].

Since, as discussed above, spatial pileup tends to result in multiple, clustered entries with overlapping neighborhoods, we may collect all  $M$  such entries to form a combined data vector

$$\mathbf{g} = \bigcup_{j=1}^M \mathbf{S}_{k_j}. \quad (23)$$

To implement a maximum-likelihood approach, we seek the number of photons  $N$  with energy and location attributes  $\mathbf{A}_i = [E_i, \mathbf{r}_i, z_i]$  which have the highest probability of creating the data vector  $\mathbf{g}$ :

$$(\mathbf{A}, N) = \arg \max p(\mathbf{g} | \mathbf{A}_1, \mathbf{A}_2, \dots, \mathbf{A}_N, N). \quad (24)$$

The probability distribution in (24) can be derived from knowledge of the response function  $f$  in (20), an approximate

expression for measurement noise, and treatment of  $N$  as a random variable governed by Poisson statistics. Though in principle the response function can be derived from electrostatics for ideal detector materials, the presence of defects in CdZnTe make it necessary to experimentally determine  $f(E, \Delta r, z)$  via careful calibration measurements [7]. For example, a well collimated gamma-ray source of known energy can be systematically scanned across the detector surface.

#### IV. IMPLICATIONS FOR DATA ACQUISITION

Spatial pileup considerations clearly have an impact on gamma-ray imaging systems based on pixellated semiconductor detectors, affecting both data acquisition and processing strategies. Successful photon counting experiments will require that the gamma-ray source intensity and the optical imaging element (typically a pinhole or collimator) efficiency be matched to keep counting rates below an appropriate maximum limit. Subsequent data processing needs to include provisions for identifying and resolving overlapping events. This inevitably involves statistical estimation from a subset of pixel signals and implies the incorporation of significant computational power as part of the instrumentation package.

Calibration procedures are a required element of any overlap separation algorithm and all individual detectors in an imaging system will need careful characterization.

#### V. ACKNOWLEDGMENTS

This work was supported by NIH Grants RO1 CA75288 and P41 RR14304.

#### VI. REFERENCES

- [1] H.H. Barrett, J.D. Eskin, and H.B. Barber, "Charge Transport in Arrays of Semiconductor Gamma-Ray Detectors," *Phys. Rev. Letters*, vol. 75(1), pp.156-159, 1995.
- [2] J.D. Eskin, H.H. Barrett, and H.B. Barber, "Signals Induced in Semiconductor Gamma-Ray Imaging Detectors," *J. Appl. Phys.*, vol. 85(2), pp.647-659, 1999.
- [3] H.B. Barber, H.H. Barrett, E.L. Dereniak, N.E. Hartsough, D.L. Perry, P.C.T. Roberts, M.M. Rogulski, J.M. Woolfenden, and E.T. Young, "Design for a High-resolution SPECT Brain Imager using Semiconductor Detector Arrays and Multiplexer Readout," *Physica Medica*, vol. IX(2-3), pp.135-145, 1993.
- [4] J. A. Heanue, J.K. Brown, and B.H. Hasegawa, "The Use of CdZnTe or CdTe for Emission-Transmission Computed Tomography: A Feasibility Study," *Nucl. Inst. and Meth. A*, vol 80, pp. 392-396, 1996.
- [5] J.L. Matteson, W. Coburn, F. Duttweiler, W.A. Heindl, G.L. Huszar, P.C. LeBlanc, M.R. Pelling, L.E. Peterson, R.E. Rothschild, R.T. Skelton, P.L. Hink, C. Crabtree, "CdZnTe Arrays for Astrophysics Applications," *Proc. SPIE*, vol 3115, pp. 160-175, 1997.
- [6] D.G. Marks, H.B. Barber, H.H. Barrett, E.L. Dereniak, J.D. Eskin, K.J. Matherson, J.M. Woolfenden, E.T. Young, F.L. Augustine, W.J. Hamilton, J.E. Venzon, B.A. Apotovsky, and F.P. Doty, "A 48x48 CdZnTe Array with Multiplexer Readout," *IEEE Trans. Nuc. Sci.*, vol. 43, pp.1253-1259, 1996.
- [7] D.G. Marks "Estimation Methods for Semiconductor Gamma-Ray Detectors," *University of Arizona Ph.D Dissertation*, 1999.
- [8] We use the notation
 
$$\iint_{\infty} d^2 r = \int_{-\infty}^{\infty} \int_{-\infty}^{\infty} dx dy$$
- [9] H.H. Barrett, T. White, and L.C. Parra, "List-mode Likelihood," *J. Opt. Soc. Am. A*, vol. 14(11), pp. 2914-2923, 1997.
- [10] L.C. Parra and H.H. Barrett, "List-mode Likelihood: EM Algorithm and Image Quality Estimation Demonstrated on 2-D PET," *IEEE Trans. Med. Imag.*, vol. 17(2), pp. 228-235, 1998.
- [11] Special provisions must be made for pixels at the detector boundary.